Nanoscale

PAPER

View Article Online
View Journal | View Issue

Cite this: *Nanoscale*, 2017, **9**, 6929

Multilayered intercalation of 1-octanol into Brodie graphite oxide†

Alexey Klechikov,[a] Jinhua Sun,[a] Igor A. Baburin,[b] Gotthard Seifert,[b] Anastasiia T. Rebrikova,[c] Natalya V. Avramenko,[c] Mikhail V. Korobov[c] and Alexandr V. Talyzin*[a]

Multilayered intercalation of 1-octanol into the structure of Brodie graphite oxide (B-GO) was studied as a function of temperature and pressure. Reversible phase transition with the addition/removal of one layer of 1-octanol was found at 265 K by means of X-ray Diffraction (XRD) and Differential Scanning Calorimetry (DSC). The same transition was observed at ambient temperature upon a pressure increase above 0.6 GPa. This transition was interpreted as an incongruent melting of the low temperature/high pressure B-GO intercalated structure with five layers of 1-octanol parallel to GO sheets (L-solvate), resulting in the formation of a four-layered structure that is stable under ambient conditions (A-solvate). Vacuum heating allows the removal of 1-octanol from the A-solvate layer by layer, while distinct sets of (00ℓ) reflections are observed for three-, two-, and one-layered solvate phases. Step by step removal of the 1-octanol layers results in changes of distance between graphene oxide planes by ~4.5 Å. This experiment proved that both L- and A-solvates are structures with layers of 1-octanol parallel to GO planes. Unusual intercalation with up to five distinct layers of 1-octanol is remarkably different from the behaviour of small alcohol molecules (methanol and ethanol), which intercalate B-GO structure with only one layer under ambient conditions and a maximum of two layers at lower temperatures or higher pressures. The data presented in this study make it possible to rule out a change in the orientation of alcohol molecules from parallel to perpendicular to the GO planes, as suggested in the 1960s to explain larger expansion of the GO lattice due to swelling with larger alcohols.

Received 13th March 2017,
Accepted 25th April 2017

DOI: 10.1039/c7nr01792h

rsc.li/nanoscale

Introduction

Graphite oxides (GOs) recently attracted enormous attention due to their ability to disperse as single sheets in various polar solvents to produce graphene oxide. The unique properties of graphene oxide multilayers were demonstrated as promising for a variety of applications, *e.g.* for the preparation of mechanically strong papers,[1] membranes for separation of gas and liquid mixtures,[2–8] nano-filtration,[9,10] and water desalination.[11,12]

The properties of graphite oxide depend very strongly on the synthesis method.[9] Currently, the most commonly studied methods are: the Brodie method (historically the earliest),[13] which involves oxidation of graphite with sodium chlorate and fuming nitric acid, the Staudenmaier method with H_2SO_4 added to the Brodie method reagents,[14] and the Hummers method, where oxidation is performed with H_2SO_4, $NaNO_3$, and $KMNO_4$. The latter method with many modifications is the most commonly used in studies of GO chemistry and in the production of various materials. However, Brodie GO (B-GO) was recently demonstrated to exhibit some unique properties that Hummers GO (H-GO) lacks, *e.g.* selective sorption of alcohols from water–alcohol mixtures[9] and distinctly different solvation and hydration properties.[9,15,16]

Graphite oxides provide enormous possibilities for chemical modification, *e.g.* the preparation of materials with porous structures using pillaring molecules.[17–19] Pillared GO materials with high surface areas could be useful for many possible applications, *e.g.* gas storage,[18] materials for supercapacitors,[20] and membranes.[21] The main strategy for creating pillared porous GO materials is a three step treatment: (1) expanding a pristine GO lattice by swelling in an appropriate solvent, (2) insertion of pillars in the dissolved state and their attachment to graphene oxide planes, and (3) removing solvent while the pillars prevent graphene oxide from restacking into the pris-

[a]*Umeå University, Department of Physics, S-90187 Umeå, Sweden. E-mail: alexandr.talyzin@umu.se*
[b]*Technische Universität Dresden, Theoretische Chemie, Bergstraße 66b, 01062 Dresden, Germany*
[c]*Department of Chemistry, Moscow State University, Leninskie Gory 1-3, Moscow 119991, Russia*

† Electronic supplementary information (ESI) available: Sketch of tentative phase diagram for B-GO-Octanol system, additional XRD data. See DOI: 10.1039/c7nr01792h

tine structure.[18] It is obvious that expansion of the GO structure by swelling is the limiting factor with respect to the size of the pillaring molecules. Therefore, the understanding and control of GO swelling is of major interest for the preparation of pillared structures.

The intercalation of polar solvents is one of the most remarkable properties of GO. The hydrophilic nature of GO has already been reported in very early studies,[22] while by the 1960s it was already well known that GO swells in polar solvents with expansion of the interlayer distance from 6–7 Å to 40–50 Å depending on the molecular size and the amount of intercalated solvent.[23,24] Perhaps the most studied GO solvates by now are those with alcohols. Previous studies revealed that B-GO is intercalated with one layer of methanol, ethanol, and propanol under ambient conditions (in excess of solvent), while an increase in pressure or a decrease in temperature leads to reversible phase transition into a two-layered solvate phase.[15,25–29] Similar phase transitions were also found for many other polar solvents (*e.g.* acetone, acetonitrile, DMF, and dioxolane[30]), while H-GO exhibits much larger expansion of the lattice and gradual changes in the interlayer distance upon pressure and temperature variations due to the effects of interstratification and intrastratification.[8,15] The step-like changes in the number of intercalated solvent layers make B-GO an important model system for understanding GO swelling and the structure of swollen GO states. One of the main difficulties in structural characterization of GO solvates is the disordered structures: no additional reflections in XRD are observed from GO functional groups and intercalated solvent molecules, thus information is mostly restricted to the distance between graphene oxide layers.

Surprisingly little is known about intercalation of GO with alcohols other than methanol, ethanol, and propanol.[15,25,29,31,32] However, a careful literature search reveals that several extensive studies of GO swelling in a variety of alcohols were performed in the 1950s and 60s.[24,33] These studies seem to be undeservingly forgotten, while the reported anomalies are not currently understood. Swelling of GO in alcohols with progressively larger sizes of molecules (up to 18 carbon atoms) was demonstrated to result in an increase in the interlayer distance of GO of up to ~50 Å. However, rather non-trivial dependence of the lattice expansion on the size of the alcohol molecule was found. For the smallest alcohols, an increase in interlayer distance of ~2.5 Å was reported,[24] while for butanol and pentanol, the structural expansion is significantly greater (7–9 Å). The expansion is even larger for alcohols with longer carbon chains.[23] D. MacEwan and J. Cano-Ruiz[23] explained this change, speculating that alcohol molecules with less than four carbon atoms are intercalated parallel to the graphene oxide sheets (alpha-phase). For molecules with a higher number of carbon atoms, the orientation of inserted molecules was suggested to change from "lying down" to "standing up" (beta-phase). Later studies by the same group also demonstrated that a GO structure intercalated with some alcohol molecules may exhibit an "alpha phase" at ambient temperature while at low temperature (223 K), a "beta phase" with an expanded interlayer distance is found.[23] In principle, multilayered graphene oxide materials intercalated with a standing up orientation of long chain hydrocarbons are known, as reported *e.g.* for ionically bonded alkylammonium molecules.[34]

However, transitions between the alpha and beta phases of GO in higher alcohols have not been studied until now and the standing up orientation of solvent molecules was never confirmed. Moreover, our earlier experiments with B-GO in methanol and ethanol provided evidence for the different natures of the low temperature and ambient-temperature phases being connected to the insertion/deinsertion of additional solvent layers.[25] Thus, the true nature of GO solvate phases with larger alcohol molecules remained unclear until now. It is worth noting that almost all the previous studies were based on XRD data, *i.e.* only the evolution of the interlayer distances in swollen B-GO was discussed. The amounts of the intercalated solvents (sorptions) were not known and were not taken into account.

In this study, we considered the formation of intercalated phases of GO and phase transitions between them using the temperature dependencies of both interlayer distances and sorptions in swollen B-GO. We report that B-GO immersed in excess of liquid 1-octanol exhibits an unusual structure with four layers of solvent intercalated parallel to the graphene oxide planes. The B-GO/1-octanol solvates are surprisingly stable, and pristine B-GO could not be recovered even after prolonged drying of the sample under ambient conditions. Phase transition to a five-layered structure is observed in the B-GO/excess 1-octanol system at lower temperatures or at high pressure. The 1-octanol can be removed from the four-layered B-GO solvate layer by layer using evaporation of solvent under vacuum at ambient and elevated temperatures. Our experiments demonstrate that higher alcohols provide a huge expansion of the GO lattice, which can be controlled in a precise way. This opens a possibility for the preparation of a next generation of pillared GO structures with possible applications as *e.g.* molecular sieves, membranes for nano-filtration, or gas separation.

Experimental

Brodie GO was synthesized by the original procedure[13] using two oxidation steps that resulted in a yellow powder with C/O = 2.55 (at%) as determined by X-ray Photoelectron Spectroscopy (XPS). This corresponds to the formula $CO_{0.39}$ and a molar mass of ~18, which was used for quantitative estimation of sorption. Some uncertainty in the molar mass estimation is always present for non-stoichiometric GO materials due to hydrogen from hydroxyl groups, residual water, and traces of oxidants used in synthesis. Material from the same batch was characterized in more detail in our earlier studies[30] and this is very similar to the samples of B-GO produced by Dr T. Szabo, which were used in our previously published experiments on B-GO swelling.[9,15,31] XRD data were collected using a Panalytical X'Pert Diffractometer with CuKα radiation. Cooling

and heating were performed using a TTK stage with thermal equilibration being achieved for a few minutes for every step. The typical recording time was 20–30 min per pattern. High-pressure experiments were performed using a Diamond Anvil Cell with a 0.6 mm culet and a stainless-steel gasket. Powder of GO and liquid 1-octanol in excess amount were loaded into a ~0.3 mm hole with a ruby ball and a piece of gold wire for pressure calibration. The pressure was increased gradually, and XRD patterns were recorded for every step during compression and decompression. XRD patterns were recorded from graphite oxide samples using synchrotron radiation at the PSICHE beamline (SOLEIL), with a wavelength of λ = 0.4859 Å, using a MARE Research image plate detector. The two-dimensional XRD patterns were integrated using Dioptase 3.1 software.

Sorption measurements at T = 298 ± 1 K were performed using an isopiestic (ISP) method. Equilibration of B-GO with 1-octanol vapor persisted until the weight of GO saturated with 1-octanol became constant (5–10 days). The sorption at melting temperature, T_m, of 1-octanol (257 ± 2 K[35]) was studied using DSC traces collected in B-GO/1-octanol systems. The weight of free solvent in direct contact with B-GO was determined from the area of the melting peak at T_m. Subtracting this weight from the total weight of the solvent in the system provides the amount of solvent sorbed (see ref. 26 for more details). DSC traces were also used to characterize phase transformations in B-GO saturated with 1-octanol. A DSC-30 TA from Mettler was used for measurements. The quantitative measurements rely on heating traces with a scanning rate of 5 K min^{-1}.

Results

Immersion of B-GO in excess amount of liquid 1-octanol under ambient conditions results in immediate expansion of the lattice from 6.7 to 23.4 Å. The B-GO/1-octanol solvate shows much better lattice ordering as is evident from a sharp decrease in the FWHM for the (001)-reflection (0.09 degrees compared to 0.43 degrees for solvent-free BGO) and an extended set of reflections from the (00ℓ) set (Fig. 2S in the ESI†). The B-GO precursor powder exhibits a weak peak from (002) and no higher order reflections, while B-GO/1-octanol shows a set of peaks with ℓ up to five. An increase in the B-GO interlayer distance by ~18 Å provides evidence of multilayered intercalation of 1-octanol. However, no direct information about the orientation of 1-octanol molecules can be extracted from the XRD data. Similarly to GO/solvent systems observed earlier,[25,36] no additional reflections due to 1-octanol intercalation are found in XRD patterns of B-GO/1-octanol. The 1-octanol molecules are completely disordered, reflecting the strong disorder of the GO layers. The only information provided by XRD is the interlayer distance provided by the 00ℓ-reflections. Considering that even the structure of the GO precursor is strongly disordered and uncertain relative to the composition of oxygen functionalities, it is impossible to build up exact structural models of GO/1-octanol. The experimentally observed interlayer distance requires multilayered intercalation of 1-octanol but is compatible with several possible orientations of 1-octanol molecules relative to the GO planes. Two possible structural models with different orientations of 1-octanol molecules are illustrated in Fig. 1. The first model assumes intercalation of four 1-octanol layers parallel to the GO planes (thickness of one layer is ~4.5 Å) (Fig. 1b) and the second model has two 1-octanol layers in a perpendicular orientation (Fig. 1a).

Compelling evidence of multilayered intercalation of 1-octanol into the GO structure was obtained by experiments with cooling of the B-GO/1-octanol sample as evidenced by XRD and DSC data analysis.

DSC scans performed with B-GO/1-octanol samples of various compositions showed no anomalies above ambient temperatures. However, below ambient temperatures, DSC scans exhibited not only a peak due to solvent freezing/melting but also a sharp peak due to phase transition, suggestively connected to insertion/deinsertion of an additional 1-octanol layer (Fig. 2).

Similar phase transitions were found in our previous studies on B-GO immersed in several polar solvents, including smaller alcohol molecules: methanol and ethanol.[15,25,26] However, the enthalpy of the transition observed for B-GO/1-octanol is remarkably higher (~25 J g^{-1} B-GO compared to *e.g.* ~9 J g^{-1} B-GO for methanol,[25] see Table 1).

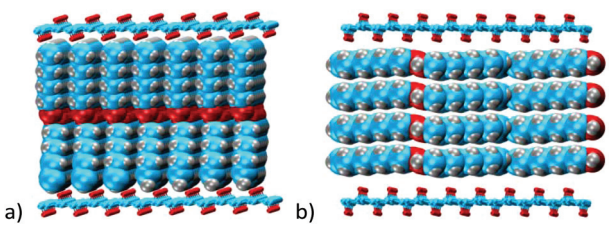

Fig. 1 Simplified structural models simulated for GO/1-octanol phases found under ambient conditions: (a) 1-octanol intercalated with perpendicular orientation and (b) 1-octanol orientation parallel to GO. Colors of atoms are: blue for carbon, red for oxygen, and gray for hydrogen.

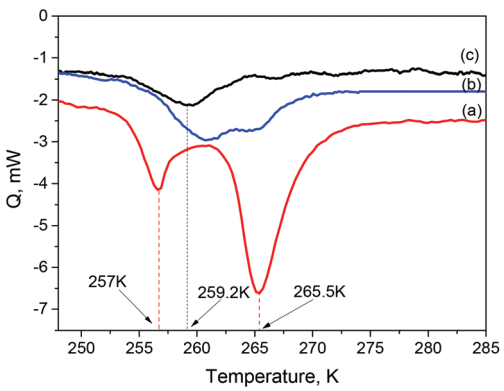

Fig. 2 Typical DSC heating traces for the binary system B-GO/1-octanol with different compositions (mol mol^{-1}): (a) *n*Oct/*n*B-GO = 0.17, which corresponds to excess liquid solvent, (b) *n*Oct/*n*B-GO = 0.14, and (c) *n*Oct/*n*B-GO = 0.12.

Table 1 Thermodynamics of reaction (1), B-GO (*S*)*n* → B-GO (*S*)*m* + (*n* − *m*) *S*, in the binary systems B-GO − *S*. The columns from left to right are: name of solvent (*S*); molar compositions for low temperature (*n*) (found using DSC method) and ambient-temperature phases (*m*) (isopiestic method); difference in interlayer distance due to insertion/deinsertion of solvent layer (Δ*d*); sorption in one layer, expressed in volumetric units or "volume of a layer" ($V_{l,\ solv}$); temperature of phase transition (T_{tr}); enthalpy of transition (Δ*H*); entropy of phase transition (Δ*S*)

Solvent (*S*)	*n* (m)[a] (±0.015)	Δ*d*, Å	$V_{l,\ solv}$, (ml g^{-1} B-GO)	T_{tr}, K	Δ*H*, J g^{-1} B-GO, (J mol^{-1})	Δ*S*, J K^{-1} g^{-1} B-GO, (J K^{-1} mol^{-1})	Ref.
1-Octanol	0.15 (0.12)	3.5[b] (4.5)	0.29	266	25 ± 6 (450)	0.09 (1.62)	This work
Methanol	0.30 (0.17)	3.3	0.36	285	9 ± 6 (162)	0.03 (0.54)	25 and 26
Acetonitrile	0.23 (0.11)	3.5	0.35	294	12 ± 6 (216)	0.04 (0.72)	25 and 26
DMF	0.18 (0.10)	4.4	0.27	315	7 ± 6 (126)	0.02 (0.36)	25 and 26

[a] For B-GO, the molecular mass was taken to be 18 u. [b] Δ*d* in temperature induced reaction (1), in round brackets – the same parameter for pressure induced reaction.

Insertion and deinsertion of solvent at the point of the phase transition can be demonstrated by analyzing DSC traces recorded from GO samples loaded with different amounts of 1-octanol expressed as the molar ratio *n*Oct/*n*B-GO.

The trace (a) in Fig. 2 was recorded for a sample with a molar ratio of *n*Oct/*n*B-GO = 0.17, which provides a significant excess of solvent as evidenced by detection of an endothermic feature at 257 K (melting of 1-octanol) and a second peak at ~265 K due to deinsertion of some 1-octanol from the GO structure. This phase transition corresponds to the incongruent melting of the low-temperature phase (L-solvate) with the formation of the ambient temperature solvate (A-solvate). The incongruent melting is described by the following reaction:

$$\text{B-GO}(C_8H_{18}O)_n \rightarrow \text{B-GO}(C_8H_{18}O)_m + (n-m)C_8H_{18}O\ (\text{liq}) \quad (1)$$

The enthalpy of transition (1) was calculated from the area of the peak at 265 K (25 J G^{-1}).

The compositions of L-solvate and A-solvate were estimated using DSC and ISP data, respectively (see Tables 1 and 2). Traces (b) and (c) in Fig. 2 were recorded using samples with an amount of 1-octanol that is close to the composition of saturated L-solvate. In this case, some liquid solvent is present in the system under loading conditions and at ambient temperature but all available liquid solvent is sorbed by the B-GO with formation of some unsaturated phase at the point of phase transition into L-phase.

No peaks due to the freezing and melting of solvent will be observed for the samples due to the absence of solvent excess in the given temperature interval. Analysis of traces (b) and (c) (*n*Oct/*n*B-GO = 0.14 and *n*Oct/*n*B-GO = 0.12, respectively) provides evidence for the existence of some solvates with compositions between those of L- and A-solvate. However, the peaks observed for traces (b) and (c) are weak and poorly resolved.

A sketch of the binary phase diagram for B-GO/1-octanol is provided in the ESI.† When *n*Oct/*n*B-GO ratios were below 0.11, no peaks could be observed in the DSC traces since all the 1-octanol present in the system was already sorbed by B-GO at ambient temperature. No excess 1-octanol is available then for additional insertion at lower temperature. The compositions of L- and A-solvates were determined using a DSC method as *n*Oct/*n*B-GO = 0.15 and *n*Oct/*n*B-GO ≥ 0.10, respectively. The composition of A-solvate was directly verified using an isopiestic method. Sorption of 1-octanol vapor under ambient conditions is slow but saturation eventually occurs at a composition of *n*Oct/*n*B-GO = 0.12.

The nature of the DSC anomaly at 265 K was verified using *in situ* XRD on a B-GO/1-octanol sample. The temperature dependence of *d*(001) shown in Fig. 3 shows a difference between ambient temperature and low temperature states of ~4.5 Å. The change in the interlayer distance of B-GO is consistent with the insertion of one 1-octanol layer in parallel orientation. Note that this transition is not correlated with the freezing of liquid 1-octanol.

A similar phase transition was also observed upon compression of B-GO in excess 1-octanol at ambient temperature (Fig. 4). Reflections from both the ambient-pressure and high-pressure phases are observed at 0.6 GPa (23.66 Å and 27.91 Å, respectively), and at higher pressures, the peak from the low-pressure phase becomes progressively weaker and shifts to higher angles. The phase transition is reversible and the pristine ambient-pressure phase was recovered after decompression.

Table 2 Sorption of polar solvents into B-GO. The columns from left to right are: name of solvent; melting temperature of solvent ™; composition of solvate at 298 K; composition of low temperature solvate at the temperature of solvent melting, T_m; difference between ambient temperature d_{298} and solvent-free sample (d_0 = 6.25 Å), and difference between *d*(001) at the melting point of the solvent (T_m) and solvent-free sample (d_0)

Solvent	T_m, K	T = 298 K, g g^{-1} (mol mol^{-1})	$T = T_m$, g g^{-1} (mol mol^{-1})	$d_{298} - d_0$; ($d_{T_m} - d_0$), A	Ref.
1-Octanol	257	0.88 ± 0.05 (0.12)	1.10 ± 0.05 (0.15)	17 (21.5)	This work
CH_3OH	175.3	0.31 ± 0.07 (0.18)	0.55 ± 0.04 (0.30)	2.83 (5.62)	25 and 26
CH_3CN	229.3	0.25 ± 0.02 (0.11)	0.53 ± 0.04 (0.23)	2.92 (6.07)	25 and 26
DMF	212.8	0.41 ± 0.05 (0.10)	0.74 ± 0.03 (0.18)	—	25 and 26

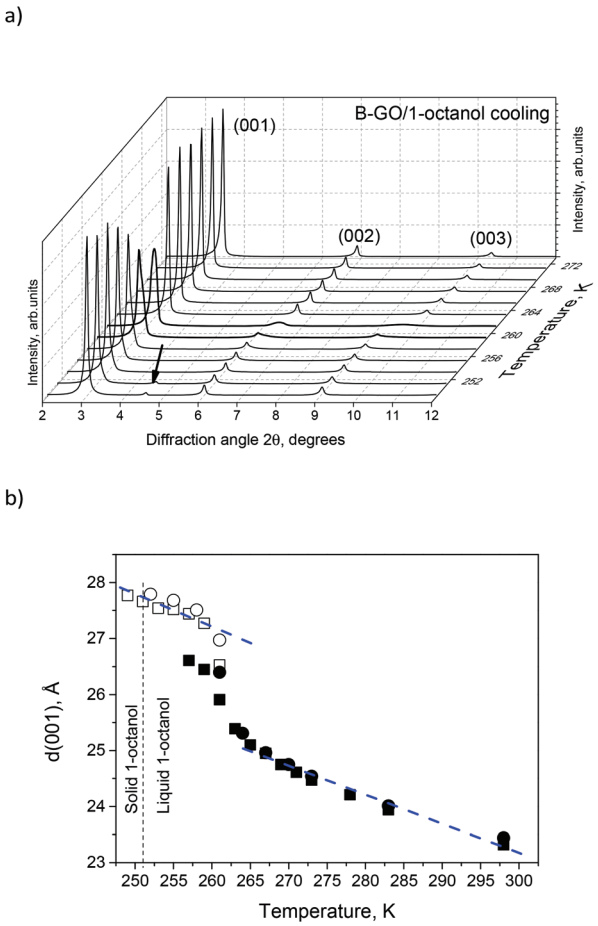

Fig. 3 (a) Diffraction patterns (CuKα radiation) recorded for a B-GO sample immersed in excess liquid 1-octanol in the temperature region of the phase transition. Emboldened patterns are for the temperature region where low temperature and high-temperature phases coexist. (b) Interlayer distance of B-GO shown for cooling (■) and heating (●) parts of the temperature cycle. Filled symbols correspond to the ambient-temperature phase and opened symbols to the low-temperature phase. The arrow shows the reflection from solid 1-octanol.

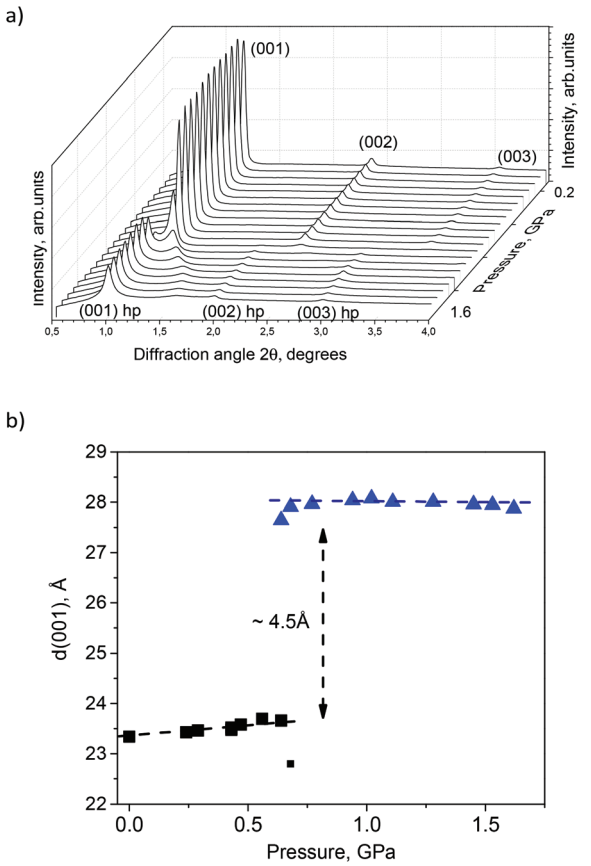

Fig. 4 X-ray diffraction patterns recorded for B-GO/1-octanol sample under high pressure conditions in DAC using synchrotron radiation (λ = 0.4859 Å).

The difference between $d(001)$ at ambient pressure and in the high-pressure phases is ~4.5 Å, which corresponds to the size of the 1-octanol layer in parallel orientation to the GO planes. It should be noted that a sharp step-like change observed for the B-GO/1-octanol structure at high pressures is different compared to cooling experiments, where a step-like increase in $d(001)$ of ~2.5 Å is observed against the background of gradual change (Fig. 3). The gradual shift in $d(001)$ was previously observed for B-GO immersed in water but not in alcohols and was assigned to the effects of interstratification.[15,37]

A gradual change in $d(001)$ was also observed for B-GO immersed in excess 1-octanol upon heating, with a decrease to about 20.3 Å at 350 K (Fig. 1S in ESI†).

Assuming the thickness of one 1-octanol layer to be 4.5 Å, the B-GO/1-octanol solvate phase observed under ambient conditions corresponds to the intercalation of four layers and three 1-octanol layers at 350 K.

Further evidence of the layered structure of B-GO/1-octanol solvates was obtained by analysis of XRD data recorded during solvent evaporation under vacuum conditions (Fig. 5). The 1-octanol has rather low vapor pressure under ambient conditions and air-drying of B-GO/1-octanol is rather slow. Therefore, we performed *in situ* XRD experiments with drying of the B-GO/1-octanol sample under vacuum and heating to 373 K. As shown in Fig. 5, the sample exposed to a vacuum at 298 K exhibited an additional set of (00ℓ) peaks with a ~4.5 Å smaller interlayer distance, while heating resulted in further loss of solvent. Analysis of XRD patterns recorded at different temperatures allows the identification of distinct B-GO/1-octanol phases with interlayer distances that correspond to one-layered (~9.9 Å), two-layered (14.6 Å), and three-layered (19.4 Å) solvate phases. The data shown in Fig. 5 provide compelling evidence for multilayered intercalation of 1-octanol with the orientation of molecules parallel to the B-GO planes.

Discussion

The experiments presented above allow a new interpretation to be provided for an anomaly in GO/alcohol swelling reported about sixty years ago.[23,24] The values of the interlayer distances

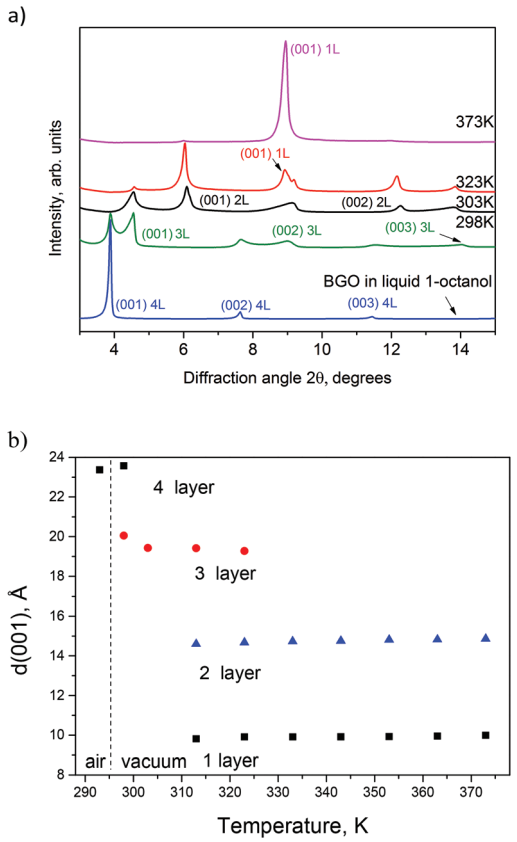

Fig. 5 (a) XRD data recorded for B-GO/1-octanol sample in the process of drying under vacuum conditions at elevated temperatures (CuKα radiation). A reference pattern recorded from a B-GO sample in liquid 1-octanol is shown at the bottom. Indexing is shown for phases with 4 to 1 layers of inserted 1-octanol (4L, 3L, 2L, and 1L). (b) Interlayer distance for distinct GO/1-octanol phases with one to four intercalated solvent layers.

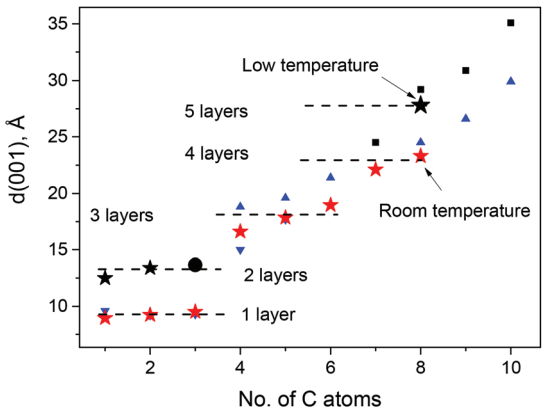

Fig. 6 Summary of data related to interlayer distance of B-GO intercalated with alcohol molecules of different lengths. Star symbols show data obtained in this study for B-GO in various alcohols (ref. 31 data used for methanol, ethanol, and propanol) at ambient temperature (★) and low temperature (★). Data from ref. 24 (▼) and ref. 23 (▲) are for ambient temperature and (■) for 223 K, ref. 29 data for propanol (●) at 240 K.

for B-GO/1-octanol found in our experiments are in good agreement with those reported in ref. 23 for both ambient and low-temperature phases (Fig. 6), especially taking into account the progress in XRD instrumentation during the last half century. However, our results explicitly demonstrate that the compositions of these two phases are different, thus ruling out suggestions about the changes in the orientation of 1-octanol molecules as a reason for the observed difference. DSC data explicitly imply that additional 1-octanol is intercalated into the B-GO structure at lower temperatures.

Tables 1 and 2 show summary of data on incongruent melting (reaction (1)), which are compared with incongruent melting transitions in systems of B-GO with other polar solvents.

The phase transition between L- and A-GO/1-octanol solvates is similar in this respect to the phase transitions observed previously for one- and two-layer solvates of B-GO.[25,26] The data obtained in this study for the phase transition between L- and A-GO/1-octanol solvates are compared in Table 1 with the data obtained previously for similar transitions between two- and one-layer solvates of B-GO.[25,26] Two parameters shown in Table 1 were used to characterize a solvent "layer" intercalated into the B-GO structure, namely the increase in the interlayer distance and the "volume of a layer", $V_{l,\ solv}$, calculated from sorption data.

As was demonstrated in ref. 26, $V_{l,\ solv}$ is a parameter of a layer that is similar for several tested solvents. Table 1 shows that both Δd and $V_{l,\ solv}$ are similar for all systems cited here, confirming that one layer of the solvent is removed in the course of the incongruent melting (1). It could be stated that the concept of a "layer", though being no more than a rough approximation, provides reasonable agreement with experimental data.

It is also worth mentioning that the entropy of reaction (1) (column 7, Table 1) for 1-octanol is higher. This is clear evidence that the type of the transition in the case of 1-octanol may be different compared to the other systems shown in Table 1.

The phase transitions of B-GO in methanol, acetonitrile, and DMF correspond to a change between one-layered and two-layered solvate phases, which approximately correlates with a two-fold change in the solvent composition (mol GO mol^{-1} solvent). This is not the case for the B-GO/1-octanol system, where the composition of the ambient-temperature phase is 0.12 and increases to 0.15 at low temperatures.

The XRD data explicitly demonstrate structures of B-GO/1-octanol with one to four solvent layers (as observed in vacuum drying experiments). The phase transition at low temperatures or high pressure is compatible with insertion of a fifth 1-octanol layer. The sorption data presented in Tables 1 and 2 are consistent with four-to-five layered solvate transitions, assuming compositions of L-solvate of 0.15 mol mol^{-1} determined using a DSC method and an A-phase composition of 0.12 mol mol^{-1} determined by an isopiestic method.

The results presented above demonstrate that the change in the orientation of the alcohol molecules cannot solely explain

the ambient temperature swelling of GO in solvents with more than four carbon atoms in the alcohol chain.

The trend is extended to 1-octanol, where the interlayer distance for the one-layer solvate phase (prepared by vacuum drying at 373 K) was found to be 9.9 Å. Note that the first layer of solvent is inserted with a smaller change in the GO lattice compared to the next layers; this is a general effect for all previously studied solvents.[25] The insertion of each additional layer of alcohol molecules into the B-GO structure should be correlated with an increase in the interlayer distance of 4–4.5 Å (14–14.5 Å). The difference between the $d(001)$ values of ambient temperature solvates of GO with propanol and butanol revealed in ref. 24 is consistent with a change from a one-layered to a two-layered solvate. However, the value of the interlayer distance reported for GO in butanol was not in good agreement with the earlier report (~14 Å)[24] and the later report (~18 Å)[23] by the same group of authors.

In order to verify the trends reported in studies from the 60s, we recorded XRD for B-GO immersed in butanol, pentanol, hexanol, and heptanol (Fig. 6). A value of $d(001)$ = 16.6 Å was found for B-GO immersed in butanol in our experiments and this probably represents a three-layered solvate structure. An interlayer distance of about 18–19 Å is expected for three-layered solvates and one of ~23–24 Å for four layered solvates. The swelling in pentanol resulted in an interlayer distance of 18.9 Å, which is close to the expected value for a three-layered solvate. Most likely, the swelling of B-GO in hexanol is also limited to three layers at ambient temperatures ($d(001)$ = 19.0 Å), while for heptanol, the value of $d(001)$ = 22.1 Å is already close to the expected interlayer distance in a four-layered solvate.

If this trend is also extended to alcohols with longer chains, the maximal lattice parameter reported in ref. 23 for GO intercalated with alcohol molecules with 18 carbon atoms (~50 Å) would correspond to the insertion of 10 solvent layers. The overall dependence of the swelling on the number of carbon atoms reported in this study seems to be rather complex and not trivial. Note that old data have been obtained on samples prepared by different method (L. Staudenmaier[14]), and lacked most of characterization, *e.g.* the precise composition of GO (C/O ratio) was not reported. The exact values of the swelling parameters were not provided in these old publications and only approximate numbers can be read from the graphical representation. Therefore, new studies that involve a broader range of alcohol molecules and graphite oxides synthesized by different methods are required to establish overall trends that include alcohols with a broad range of alkyl chain lengths over broad temperature intervals. Multilayered sorption of larger alcohols by B-GO structures is a non-trivial effect that requires further theoretical and experimental studies.

It must be emphasized that GO produced by the Hummers method does not exhibit phase transitions in ethanol and methanol (as well as all other studied solvents).[15] Only a gradual change in the interlayer distance was observed for H-GO in 1-octanol (from 23.4 Å at ambient temperature to 28.0 Å at 251 K) upon cooling. The absence of step-like phase transitions in H-GO may be explained by inhomogeneous oxidation of H-GO and the effects of interstratification and intrastratification.[8,38]

In summary, we resolved sixty years old questions related to the structure of GO/alcohol solvates, focusing on a detailed study of the B-GO/1-octanol system. It was found that 1-octanol intercalates into the B-GO lattice with the orientation of molecules parallel relative to the graphene oxide sheets and with the formation of one- to five-layered solvate structures. Maximal five-layered intercalation is observed below ~260 K at ambient temperature and at pressures over ~0.6 GPa. A four-layered B-GO/1-octanol solvate phase is found under ambient conditions while three-layered, two-layered, and one-layered solvate phases were observed in the process of vacuum drying the samples at elevated temperatures. Therefore, the interlayer distance of B-GO can be precisely tuned using a selection of alcohol molecules and temperature/pressure conditions, which makes higher alcohols attractive solvents for the preparation of pillared structures.

Acknowledgements

A. T. R., N. V. A., and M. V. K. acknowledge financial support from the RFBR (grant 15-03-02168) and from the grant for Leading Scientific Schools in Russia. A. T., I. B., and G. S. acknowledge funding from the European Union's Horizon 2020 research and innovation program under grant agreement no. 696656. A. T. thanks Carl Tryggers Stiftelse for financial support.

References

1 D. A. Dikin, S. Stankovich, E. J. Zimney, R. D. Piner, G. H. B. Dommett, G. Evmenenko, S. T. Nguyen and R. S. Ruoff, *Nature*, 2007, **448**, 457–460.
2 H. P. Boehm, A. Clauss and U. Hofmann, *J. Chim. Phys. Phys.-Chim. Biol.*, 1961, **58**, 141–147.
3 C. M. Chen, Q. H. Yang, Y. G. Yang, W. Lv, Y. F. Wen, P. X. Hou, M. Z. Wang and H. M. Cheng, *Adv. Mater.*, 2009, **21**, 3007–3011.
4 Z. T. Luo, Y. Lu, L. A. Somers and A. T. C. Johnson, *J. Am. Chem. Soc.*, 2009, **131**, 898–899.
5 H. W. Kim, H. W. Yoon, S.-M. Yoon, B. K. Ahn, Y. H. Cho, H. J. Shin, H. Yang, U. Paik, S. Kwon, J.-Y. Choi and H. B. Park, *Science*, 2013, **342**, 91–95.
6 H. Li, Z. Song, X. Zhang, Y. Huang, S. Li, Y. Mao, H. J. Ploehn, Y. Bao and M. Yu, *Science*, 2013, **342**, 95–98.
7 Y. P. Tang, D. R. Paul and T. S. Chung, *J. Membr. Sci.*, 2014, **458**, 199–208.
8 B. Rezania, N. Severin, A. V. Talyzin and J. P. Rabe, *Nano Lett.*, 2014, **14**, 3993–3998.
9 S. J. You, S. M. Luzan, T. Szabo and A. V. Talyzin, *Carbon*, 2013, **52**, 171–180.

10 R. K. Joshi, P. Carbone, F. C. Wang, V. G. Kravets, Y. Su, I. V. Grigorieva, H. A. Wu, A. K. Geim and R. R. Nair, *Science*, 2014, **343**, 752–754.
11 E. S. Bober, L. C. Flowers, P. K. Lee, D. E. Sestrich, C.-M. Wong, W. Gillam Sherman, S. Johnson and R. H. Horowitz, Research and development progress report No. 544, US Department of the Interior, reprints from the colelction of the University of Michigan Library, 1970, pp. 1–113.
12 A. Nicolai, B. G. Sumpter and V. Meuniera, *Phys. Chem. Chem. Phys.*, 2014, **16**, 8646–8654.
13 B. C. Brodie, *Philos. Trans. R. Soc. London*, 1859, **149**, 249–259.
14 L. Staudenmaier, *Ber. Dtsch. Chem. Ges.*, 1898, **31**, 1481–1487.
15 S. J. You, B. Sundqvist and A. V. Talyzin, *ACS Nano*, 2013, **7**, 1395–1399.
16 W. S. Hummers and R. E. Offeman, *J. Am. Chem. Soc.*, 1958, **80**, 1339–1339.
17 J. W. Burress, S. Gadipelli, J. Ford, J. M. Simmons, W. Zhou and T. Yildirim, *Angew. Chem., Int. Ed.*, 2010, **49**, 8902–8904.
18 G. Mercier, A. Klechikov, M. Hedenstrom, D. Johnels, I. A. Baburin, G. Seifert, R. Mysyk and A. V. Talyzin, *J. Phys. Chem. C*, 2015, **119**, 27179–27191.
19 R. Kumar, V. M. Suresh, T. K. Maji and C. N. R. Rao, *Chem. Commun.*, 2014, **50**, 2015–2017.
20 L. Li, J. J. Qiu and S. R. Wang, *Soft Mater.*, 2013, **11**, 503–509.
21 W. S. Hung, C. H. Tsou, M. De Guzman, Q. F. An, Y. L. Liu, Y. M. Zhang, C. C. Hu, K. R. Lee and J. Y. Lai, *Chem. Mater.*, 2014, **26**, 2983–2990.
22 U. F. Hofmann and A. Frenzel, *Ber. Dtsch. Chem. Ges.*, 1930, **63**, 14.
23 A. R. Garcia, J. Cano-Ruiz and D. M. C. Macewan, *Nature*, 1964, **203**, 1063–1064.
24 J. C. Ruiz and D. M. C. Macewan, *Nature*, 1955, **176**, 1222–1223.
25 S. J. You, S. Luzan, J. C. Yu, B. Sundqvist and A. V. Talyzin, *J. Phys. Chem. Lett.*, 2012, **3**, 812–817.
26 M. V. Korobov, A. V. Talyzin, A. T. Rebrikova, E. A. Shilayeva, N. V. Avramenko, A. N. Gagarin and N. B. Ferapontov, *Carbon*, 2016, **102**, 297–303.
27 A. Vorobiev, A. Dennison, D. Chernyshov, V. Skrypnychuk, D. Barbero and A. V. Talyzin, *Nanoscale*, 2014, **6**, 12151–12156.
28 A. V. Talyzin and S. M. Luzan, *J. Phys. Chem. C*, 2010, **114**, 7004–7006.
29 C. Cabrillo, F. Barroso-Bujans, R. Fernandez-Perea, F. Fernandez-Alonso, D. Bowron and F. J. Bermejo, *Carbon*, 2016, **100**, 546–555.
30 A. V. Talyzin, A. Klechikov, M. Korobov, A. T. Rebrikova, N. V. Avramenko, M. F. Gholami, N. Severin and J. P. Rabe, *Nanoscale*, 2015, **7**, 12625–12630.
31 A. V. Talyzin, B. Sundqvist, T. Szabo, I. Dekany and V. Dmitriev, *J. Am. Chem. Soc.*, 2009, **131**, 18445–18449.
32 F. Barroso-Bujans, S. Cerveny, R. Verdejo, J. J. del Val, J. M. Alberdi, A. Alegria and J. Colmenero, *Carbon*, 2010, **48**, 1079–1087.
33 C. Delpino, A. Ramirez and J. Canoruiz, *Nature*, 1966, **209**, 906–907.
34 M. Mauro, M. Maggio, V. Cipolletti, M. Galimberti, P. Longo and G. Guerra, *Carbon*, 2013, **61**, 395–403.
35 J. Carper, *Library J.*, 1999, **124**, 192–300.
36 A. Klechikov, J. C. Yu, D. Thomas, T. Sharifi and A. V. Talyzin, *Nanoscale*, 2015, **7**, 15374–15384.
37 A. V. Talyzin, S. M. Luzan, T. Szabo, D. Chernyshev and V. Dmitriev, *Carbon*, 2011, **49**, 1894–1899.
38 A. V. Talyzin, T. Hausmaninger, S. J. You and T. Szabo, *Nanoscale*, 2014, **6**, 272–281.